AIP | Journal of Applied Physics

Electrical conduction in ternary semiconductor Ga5Se20Te75 thin films

V. Damodara Das, K. S. Raju, and A. Bhaskaran

Electrical conduction in ternary semiconductor $Ga_5Se_{20}Te_{75}$ thin films

V. Damodara Das[a)]
Thin Film Laboratory, Department of Physics, Indian Institute of Technology, Madras, Madras 600036, India

K. S. Raju and A. Bhaskaran
Department of Crystallography and Biophysics, University of Madras, Guindy Campus, Madras 600025, India

(Received 19 September 1994; accepted for publication 12 May 1995)

Different thickness thin films of the ternary alloy $Ga_5Se_{20}Te_{75}$ have been vacuum deposited on clean glass substrates held at room temperature at a very fast rate. The film resistance has been measured as a function of temperature during two cycles of heating and cooling. It has been found that the resistance-temperature (R-T) variation of the films during first heating and cooling is different, the R-T curve during heating lying above the R-T curve during cooling in the case of thinner films and below in the case of thicker films. There are two possible explanations for the difference in resistance variation during heating and cooling and between the thinner and thicker films. The first is due to the semiconducting nature of the material and the second is due to the removal of frozen-in defects and/or change in concentration depth profile. In addition to these, the phenomenon of self-annealing can also take place in thicker films. Log resistance vs reciprocal temperature plots are found to be linear, indicating activated conduction in the film material. It has also been found that resistance vs reciprocal thickness plot is near-linear as expected from the classical size effect theories. X-ray diffraction has established that the films are single phase. X-ray photoelectron spectroscopic (XPS) studies have revealed that the film surface is enriched with tellurium such as TeO_2 [BE ($3d_{5/2}$)=577 eV], in addition to the presence of selenium [BE ($3d$)=55.5 eV] and gallium in traces [BE ($2p_{3/2}$)=1117 eV].

I. INTRODUCTION

Some of the ternary, quaternary, and multicomponent tellurium-rich alloys are known to have nonlinear current-voltage (I-V) characteristics, and switch from the high resistance "off" state for lower applied voltages, to the low resistance "on" state for higher voltages. Thus, some of these tellurium-rich multicomponent alloys can be used as microswitches in electronic circuits to switch "on" or "off" current through different parts of the circuit where they are incorporated.[1–3] Hence, researchers are trying to discover new materials and compositions which can be used for operation as bistable devices. The point to note is that a particular material which is bistable in the bulk solid state need not necessarily behave in a similar manner as a thin film. Hence, a multicomponent alloy which is suitable as a microswitch in the bulk may not be so as a thin film microswitch.

A number of workers have investigated different tellurium-rich multicomponent alloys both in bulk and thin film form[1–13] to investigate whether these materials can be used as bistable microswitches. We have reported on the results of similar investigations on tellurium-rich binary and ternary materials like $Se_{20}Te_{80}$, $Se_{10}Bi_{10}Te_{80}$, and $Se_{10}Sb_{10}Te_{80}$ and various Se-Te alloys of different compositions.[14–16] In the present work are reported the electrical conductivity studies made on flash-evaporated tellurium-rich ternary alloy $Ga_5Se_{20}Te_{75}$ thin films as a function of thickness and during and after vacuum annealing. Also reported are the results of x-ray diffraction (XRD), EDAX, and XPS analyses of the films. The single phase nature of our $Ga_5Se_{20}Te_{75}$ alloy thin films was confirmed by XRD. EDAX was used for semiquantitative determination of film composition while XPS was used to determine the chemical state of the species.

II. EXPERIMENT

Thin films of the alloy $Ga_5Se_{20}Te_{75}$ were vacuum flash-deposited onto cleaned glass substrates held at room temperature in a vacuum of 5×10^{-5} Torr. Flash evaporation was carried out by heating small pieces of the bulk alloy of the above composition in a resistively heated basket type tantalum boat so that the material evaporated at a very fast rate. During each run, a number of "soda-lime" glass plates of size 7.5 cm×2.5 cm×2 mm were kept symmetrically above the boat on a substrate holder, so that the films on the substrates were similar. The films of lateral dimensions 1 cm×7 cm were prepared on these glass substrates using suitable masks. The perpendicular distance between the substrates and the central evaporation source was 25 cm. Films of different thicknesses were prepared in independent evaporations. During each evaporation, the material in the boat was completely evaporated, so that no alloy material was left over in the boat. For each flash evaporation, small fresh pieces of the bulk alloy were used. Flash evaporation ensures

a)Electronic mail: phy10@iitm.ernet.in

that there is no significant change in the composition of the thin film as compared to the bulk composition of the alloy due to preferential evaporation of one of the components, Se, which is very volatile. A dummy, sharp-edged film was also prepared simultaneously in each of the evaporations. It was later used for the measurement of thickness by the multiple beam interference technique.[17]

The as-grown films were mounted inside the resistance measurement setup in the vacuum chamber and the chamber was evacuated to 3×10^{-5} Torr before making the resistance measurements. The measurement technique was as follows: The glass substrate with the thin film was mounted glass side down onto a bottom copper plate. Then, thin copper foil contact pads were mechanically clamped onto the film side using copper sheet strips and screws. The contact pad areas were about 1 cm^2. The whole resistance measurement assembly was placed on an electrically heated copper hot plate inside the vacuum chamber so that the film could be heated in vacuum and its resistance measured as a function of temperature. The resistance measurement reproducibility was better than 0.1% based on the number of significant digits possible with a Kiethley DMM.

The contact area of the copper pad contacts onto the film was 1 cm^2 and the copper pad had number of layers of thin copper film which were compressible. So, good, large area contact with the deposited thin film could be achieved. Hence, the contact resistance can be taken to be negligibly small. *I*-*V* measurements were also made in both directions of current flow in the film (through the contacts) and it was found that the current-voltage variation was linear which confirmed that the contacts were ohmic. Also, all the films were made using masks and the resistance measurement setup was such that only the resistance of a fixed length of the film was measured. Thus, the errors in the linear dimensions of the films could be neglected. So, except for the thickness of the films, the other dimensions during measurements were the same for all films.

To confirm that the formed films were of single phase, x-ray diffractograms of the films were taken both before and after the resistance measurements. The presence of metal constituents in the ternary alloy was confirmed by EDAX. Thin film samples were coated with silver paste prior to EDAX measurements in a scanning electron microscope (SEM) (Cambridge type 7313).

For XPS analysis, all spectra were recorded on a Perkin Elmer 5300 XPS at a base pressure of about 10^{-9} Torr using an Al ($K_{\alpha1,2}$=1486.6 eV) x-ray source operated at 15 kV and 400 W. The spectrometer was calibrated by setting binding energies of Au $4f_{7/2}$ and Cu $2p_{3/2}$ level values to 84.0 and 932.7 eV, respectively. Multiplex spectra were collected at 45° and 60° with respect to the film.

III. RESULTS AND DISCUSSION

A. Irreversible resistance changes

Electrical resistance measurements were made during two cycles of heating and cooling on films of different thicknesses between about 400 and 3500 Å. Figure 1 shows the electrical resistance variation of two of the typical films during the first heating and cooling between the temperatures of about 300 and 500 K. Films of other thicknesses also behave in a similar way. It can be seen from the figures that the resistance variation during the first heating and cooling are different. It was noted that for thinner films, the heating curve was above the cooling curve [Fig. 1(a)], but in the case of the thicker films studied, the cooling curve was above the heating curve [Fig. 1(b)]. During the second heating and cooling cycle, the resistance variation observed during the first cycle cooling was very nearly reproduced, thus confirming that during the first cycle heating, *irreversible changes occur* in the films which change the film resistance irreversibly. As the resistance variation with temperature during the second heating-cooling cycle is nearly the same as that during the first cycle cooling, *no significant irreversible changes occur* during the second (and subsequent) heating-cooling cycles.

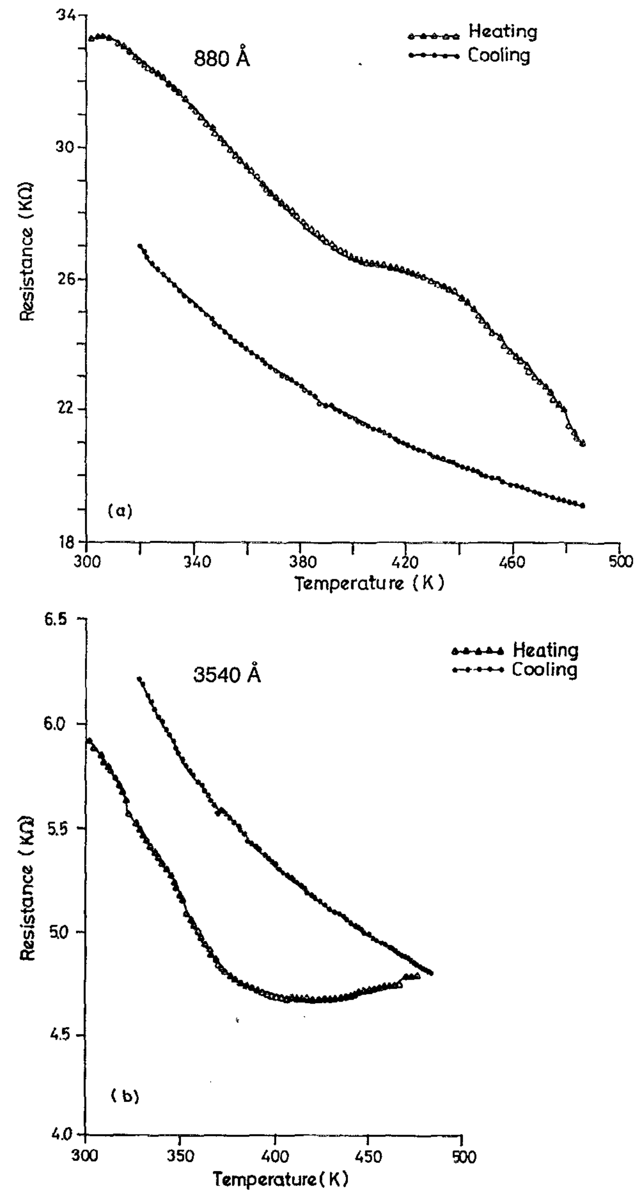

FIG. 1. Resistance variation during heating-cooling cycles of typical as-grown thin films of $Ga_5Se_{20}Te_{75}$ (thickness 880 Å and 3540 Å).

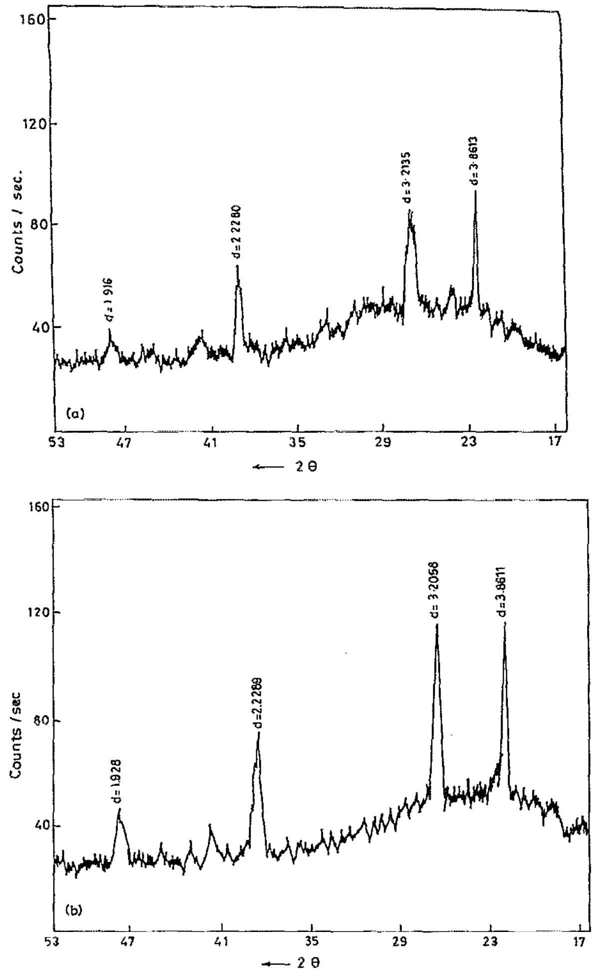

FIG. 2. (a), (b) X-ray patterns of the typical as-grown thin film before and after resistance measurements.

TABLE I. Comparison of x-ray diffractogram data of $Ga_5Se_{20}Te_{75}$ film before and after heating with the x-ray data of $Se_{20}Te_{80}$ alloy.

'd' Standard of $Se_{20}Te_{80}$ (Å)	hkl	'd' of $Ga_5Se_{20}Te_{75}$ film (Before heating) (Å)	'd' of $Ga_5Se_{20}Te_{75}$ film (After annealing) (Å)
3.849	100	3.861	3.861
3.194	101	3.213	3.206
2.297	102		
2.222	110	2.228	2.229
1.925	200	1.916	1.928
1.824	201		
1.755	112		
1.597	202		
1.455	120		
1.410	121		
1.297	212		
1.252	301		

The thermal expansion coefficient of soda-lime glass is about 9.3×10^{-6}/K and that of tellurium, the major constituent of our films is 16.75×10^{-6}/K. Hence, during heating, there will be a difference in thermal expansion between the glass substrate and the thin film. Hence, as the temperature changes, this difference in thermal expansion coefficients will lead to the development of stresses in the film. This also contributes to the total film resistance. However, it should be pointed out here that even though this contribution to the film electrical resistance changes with temperature, if we are considering only the *irreversible changes in film resistance during the initial (first) heating cycle*, this contribution is immaterial because the difference in expansion of the film material and the glass substrate exists not only during the initial heating-cooling cycle but also in the second heating-cooling and other subsequent cycles. Because during the second heating-cooling cycle (and the subsequent cycles) the resistance variation with temperature is *reproducible*, we can rule out the possibility of this difference in thermal expansion of the substrate and the thin film causing the observed *irreversible resistance changes during the initial (first) heating cycle*.

Figures 2(a) and 2(b) show the typical x-ray diffractograms obtained from the as-grown thin film (a) and from the film on which resistance measurement during one cycle of heating and cooling had been done (b). It can be seen from the figures that the diffraction peak positions do not change because of the heat treatment, and hence the film alloy composition is maintained. The d values obtained in both the cases match well with the $Se_{20}Te_{80}$ d values reported in literature (Table I).[15] Thus, except for an increase in the peak heights, indicating some amount of preferential orientations or increased crystallinity of some grains, no noticeable changes can be seen in the x-ray diffractograms. The irreversible resistance variation of the films observed during the first heating can be explained by the following.

As-grown thin films prepared by vacuum deposition, whether metallic, semiconducting, or insulating may contain a large quantity of frozen-in defects associated with occluded gas molecules from the vacuum chamber.[18–21] These defects can form due to the formation of complex molecules and clusters of defects in association with the occluded gas atoms and other interstitial atoms of the different elements of the film material and vacancies in the films. If present, these defects can increase the resistance of as-grown thin films because of the additional scattering due to these frozen-in defects. On heating, these frozen-in defects are partially or completely removed depending upon the temperatures reached during heating. This removal of defects is a continuous process which takes place throughout the heating process depending on the specimen film temperature reached at a given heating rate. Thus, as the temperature increases, the resistance starts decreasing monotonically.[21] Thus, a steep decrease in resistance with increase of temperature during heating can be explained. During the cooling process, with a decrease in temperature, the resistance monotonically increases, but not so steeply as in the case of heating. The increase of resistance with a decrease in temperature during the cooling cycle shows that the film conduction is activated as can be expected in semiconductors.

The effect of annealing of frozen-in defects during heating is to decrease the resistance to nearly half its initial re-

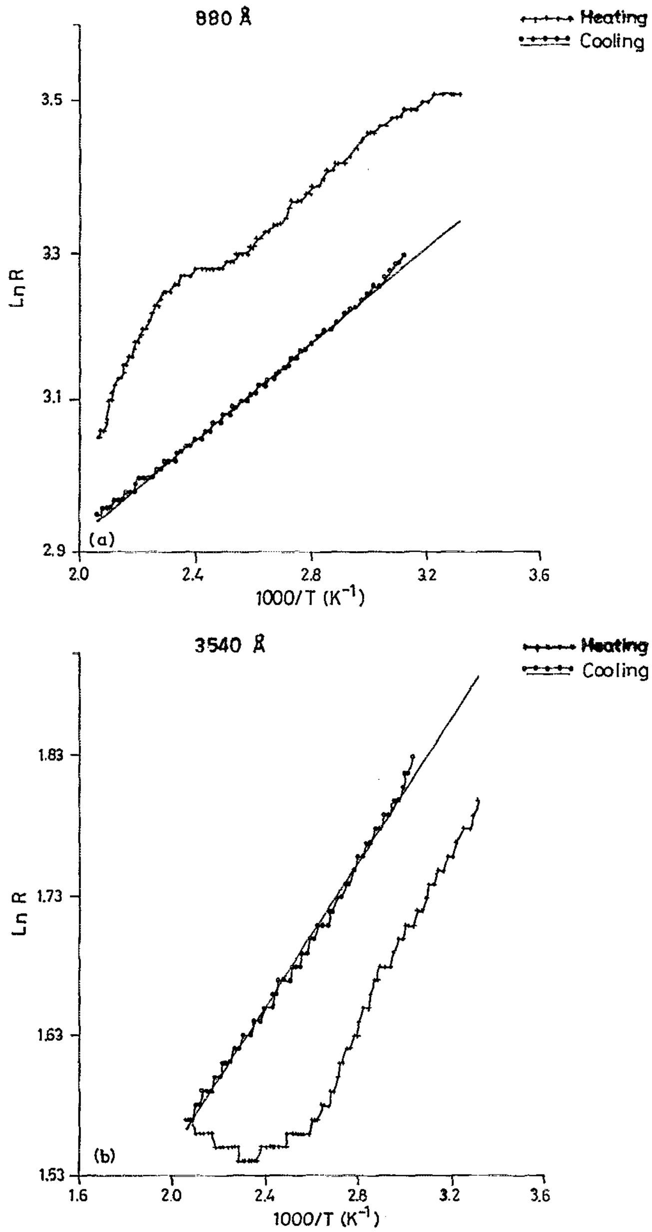

FIG. 3. Log resistance vs reciprocal temperature plots of the above films showing linearity during the cooling cycle.

sistance (of as-grown films) in a few cases. Smaller values of resistance at the lowest temperature (of 300 K) show that the resistance of the film has decreased because of the removal of frozen-in defects. The true semiconductor-like activated conduction behavior in the film can only be observed during cooling as the resistance behavior during the heating cycles is the combination of the resistance change due to the semiconducting nature of the thin film material and the resistance decrease due to defect removal.

In the case of the two thickest films, the resistance variation curve during cooling is above that during heating. This may be because thicker films require larger times (though of the same order) for deposition, and consequently allow more time for self-annealing. It is evident that to prepare a thicker film, the evaporation source has to be kept at the high temperature for a larger (say, by a factor of 3 or 4) duration of time. Hence, the radiation heat from the source falling on the thin films can raise the temperature to a higher value momentarily during the film formation itself. Therefore, the thicker film can get self-annealed. Thus, the thicker films are already self-annealed during the formation itself, and hence, heating of films during the resistance measurements does not have any significant effect because the frozen-in defects are already removed during the self-annealing. As a matter of fact, the highest temperature reached during heating of the film is sufficiently high to partially evaporate the film material so that the film resistance increases, as was found during the first heating cycle in the case of thicker films.

Because of the elevated temperature during the heating process, diffusion of atoms of the different constituent elements of the thin film takes place. This will lead to the change in the concentration profiles of various elements along the depth of the film. However, as we are experimentally effectively measuring only the "total film resistance" and not that of the individual layers, the change in depth profile of concentration of the species is not very likely to cause a significantly large irreversible change in film resistance during the first (or subsequent) heating. Hence, we may say that the major portion of the irreversible changes taking place during the initial heating are due to removal of frozen-in defects. However, it should be pointed out that the defect clusters that form in combination of occluded gas molecules consist also of vacancies and interstitials which are nothing but the atoms of the elements of the film material. Thus, the migrated material atoms during the heating process will and do combine with some of the gas molecules and vacancies to form lesser energy atom-clusters which also lead to changes in carrier scattering and hence decrease in resistance of the film. Thus, the removal of defect clusters is the general process occurring in which the migration of the material atoms and their combining with gas molecules and vacancies to form clusters of lesser energies is also one part of the process of rearrangement of atoms towards thermodynamic equilibrium.

It is worth pointing out here that we have observed similar irreversible changes in film resistance upon first heating even in elemental thin films like of bismuth and tellurium, tin, etc.[21–23] where there is no possibility of any change in depth profile. Thus, these earlier observations clearly indicate that the major change in the film resistance during first heating takes place because of the removal of atom-cluster defects formed with the occluded gas molecules, interstitial atoms of the material and vacancies in the lattice. Change in depth profile of the constituent elements causes only minor and very small changes in film resistance during the first heating.

B. Reversible temperature dependence of resistance

Figures 3(a) and 3(b) show the plots of ln R versus reciprocal temperature during both heating and cooling for the above typical thin films (calculated from the data of Fig. 1). It is seen from the figures that ln R vs $1/T$ plots are linear during the cooling cycle. Similar linearity was also observed

TABLE II. Thickness dependence of conduction activation energy.

Thickness (t) (Å)	Activation energy 'E_g' (in meV) while cooling
440	26.8
880	28.0
1340	30.8
1780	36.1
2660	26.3
3540	22.4

TABLE III. Mean free path and "infinite thickness" film resistivity as a function of temperature.

Temperature (K)	$\rho_g \times 10^{-2}$ Ω cm	l_g (Å)
350	3.98	270
400	3.49	282
450	3.21	289

in the case of other films of different thicknesses. However, ln R vs $1/T$ plots are not linear during the heating cycle except in the case of the two thickest films of thicknesses 2660 and 3540 Å.

The nonlinear behavior of ln R vs $1/T$ plots during the heating cycle indicates that in addition to the semiconducting nature of the material, removal of frozen-in defects and to some extent rearrangement of different atomic species of the film material, also contributes to the observed resistance variation. Hence, ln R vs $1/T$ plots cannot be linear. During cooling, ln R vs $1/T$ plots are linear as expected from the contribution of the semiconducting nature of the material because the nonequilibrium defects frozen-in in the films are annealed out during the first heating, and hence, do not contribute to resistance increase due to scattering of carriers.

The fact that ln R vs $1/T$ plots are linear in the case of the two thickest films both during heating and cooling supports the earlier deduction about removal of frozen-in defects during self-annealing in the case of thickest films. Also, it should be pointed out that ln R vs $1/T$ plots during cooling were nearly parallel except for the shift towards higher resistance during cooling. This fact supports the contention that in the case of the two thickest films, heating leads to partial evaporation of the material at higher temperatures of anneal, close to 500 K.

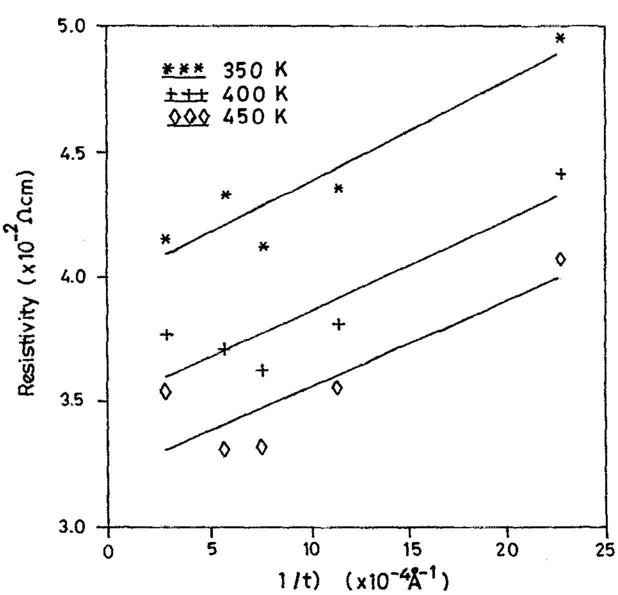

FIG. 4. Film resistivity vs reciprocal thickness plots of $Ga_5Se_{20}Te_{75}$ films at three different temperatures showing linearity.

Activation energy for conduction can be calculated from the plots of ln R vs $1/T$ during the cooling cycle in the case of all the films. The activation energy values calculated are tabulated in Table II. It is seen from the table that except for two thicker films, the activation energy of all thinner films moderately increases with an increase in thickness (from about 27 to 36 meV). This suggests that the film thickness influences the activation energy to some extent. This apparently is related to the grain size of the films as it is well known that the film microcrystallite size increases with increase in thickness up to the film continuity stage, thereafter it remains almost constant. This interpretation also possibly explains the decrease of activation energy for larger thicknesses.

C. Thickness dependence of resistivity

To investigate the effect of thickness on film resistivity (at a given temperature) of *well-annealed* thin films (so that frozen-in defects are removed from the films), the resistance values of all the films at temperatures 350, 400, and 450 K were noted from the cooling curves of resistance variation for all the films of different thicknesses. Figure 4 shows the plots of film resistivity ρ_F (calculated from the above resistance data and thicknesses and lateral dimensions of the various films) as a function of reciprocal thickness at three different temperatures of 350, 400, and 450 K. The experimental plots are shown by the symbols and the straight line plots in the figure are the linear fits of the experimental data. It is seen that the experimental points form nearly straight line plots within experimental errors.

We know that in the case of thin films, resistivity, $\rho_F = R_F(bt/l)$ [b=film breadth, l=film length, and t=film

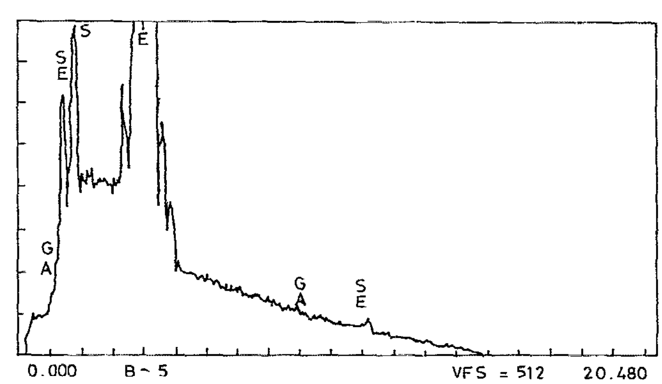

FIG. 5. EDAX pattern of a typical thin film of $Ga_5Se_{20}Te_{75}$.

TABLE IV. EDAX data of typical "$Ga_5Se_{20}Te_{75}$" thin films.

Element	K ratio	Z	A	F	At. %	Wt %	Net counts
Ga-K	0.001	0.935	1.022	0.997	0.11	0.11	151
Se-L	0.026	0.989	1.985	0.996	4.57	5.12	209
Te-L	0.664	1.084	1.016	1.000	40.35	73.13	801
Si-K	0.136	0.808	1.853	0.998	50.84	20.29	290
Na-K	0.004	0.830	4.075	0.999	4.13	7.35	65

thickness] becomes a function of reciprocal thickness ($1/t$) due to additional carrier scattering from internal and external surfaces of thin films, and also due some extent to rearrangement of different atomic species in the film.[24–28] This leads to the effect well known as the classical size effect. All the size effect models proposed predict a linear increase of film resistivity, ρ_F, with increasing reciprocal thickness. Thus, the observed linearity of the film resistivity, ρ_F vs reciprocal thickness ($1/t$) plots is as expected from the theory. From the intercepts of these plots, resistivity ρ_g, of the infinite-thickness films at different temperatures has been determined. These values are tabulated in Table III. The significance of infinite thickness film resistivity is that it approximates to bulk resistivity when the the bulk material has the same microcrystallite size (grain size) as the films have.[27]

From the slopes of these plots, assuming diffuse scattering ($p=0$), the mean free path of carriers in the films at three different temperatures has been evaluated. These are also tabulated in Table III. It is seen from the table that mean free path is the same at three different temperatures (within experimental errors which are ± 20 Å). Thus, it can be concluded that in these *well-annealed* thin films, major scattering processes are due to intergrain boundaries and film surfaces. Hence, thermal effects (lattice vibrations effects) so also scattering due to frozen-in defects do not affect significantly the mean free path in the films.

D. Chemical and compositional analysis

The EDAX of the thin film records the presence of tellurium, selenium and gallium (in traces) (Fig. 5). Table IV tabulates the concentrations of the elements obtained from the XPS analysis of the combination of the film and top few layers of the glass substrate. Since we know that the peaks of Si and Na come from the glass substrates used, we can calculate the real concentration of the elements in the films by normalizing the concentrations taking the sum of three concentrations of Ga, Se, and Te as 100. The normalized concentrations thus obtained are listed in Table V. From the values it is seen that the percentage composition of the elements incorporated in the film (Table V) agree only semiquantitatively with bulk alloy composition. Particularly, Te concentration of the film recorded from XPS is higher than the bulk concentration while the concentrations of volatile elements—Ga and Se—are lower. This can be explained by the possibility of *sublimation of the volatile components Se and Ga from the film during the XPS analysis due to the incidence of energetic radiation.*

TABLE V. Normalized "real" concentrations of the elements in the films calculated from the EDAX data.

Material	Symbol	At. % concentration
Gallium	(Ga)	0.24%
Selenium	(Se)	10.15%
Tellurium	(Te)	89.61%
Total		100.00%

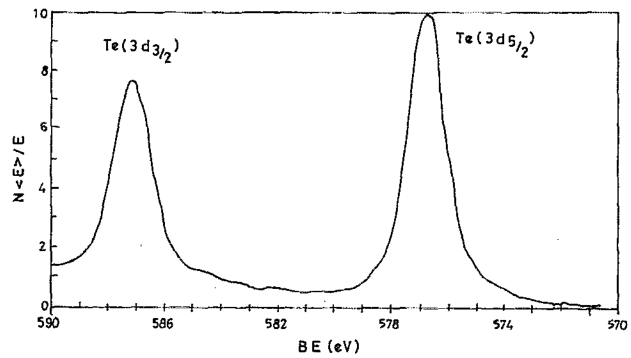

FIG. 6. XPS peaks relating to TeO_2.

From XPS it is also observed that the film surface is not homogeneous and also not of the same composition as the bulk of the thin film. At the lower angle, XPS reveals that the film surface is enriched with TeO_2 [BE $(3d_{5/2})=577$ eV] (Fig. 6), while at higher angles Te metal becomes visible. This is because TeO can be seen most likely when the oxide overlayer is of the order of 100 Å. XPS also establishes the presence of selenium BE $(3d)=55.5$ eV quite adjacent to strong sodium peak of the glass substrate [BE $(2s)=64$ eV)] (Fig. 7). The presence of gallium in traces is established by comparing the XPS peak relating to gallium [BE $(2p_{3/2})$ $=1117$ eV] in the multiplex spectra at 45° and 60° (Fig. 8). It should be mentioned that these binding energy values quoted in the present work relating the XPS peaks of the respective film constituents agree quite well with the reported values in the literature.[29] From XPS it is clear that the intensity of the Te $3d_{5/2}$ peak is much greater than the intensity of Se $3d$, which in turn is much greater than the intensity of Ga $2p_{3/2}$ which agrees semiquantitatively with the composition of the bulk alloy, i.e., atomic composition of Te(75)≫SE(20)≫Ga(5). It should also be pointed out that no

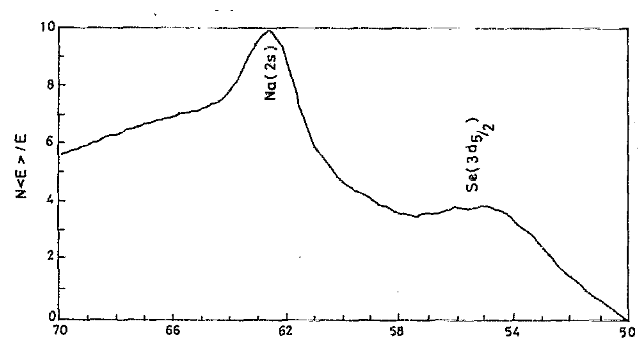

FIG. 7. XPS peaks relating to selenium.

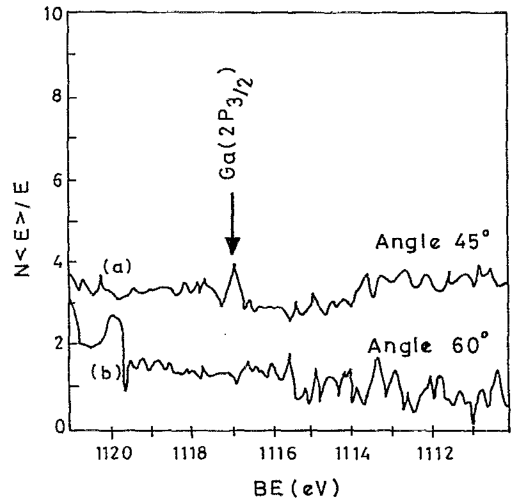

FIG. 8. XPS spectra relating to gallium [at (a) 45° and (b) 60°].

additional peaks except the four mentioned (of the alloy $Ga_5Se_{20}Te_{75}$) were seen in the x-ray diffractograms, and hence, it can be concluded that bulk of the film is free of any oxides or pure elemental materials. Only the surface has oxides (of tellurium).

IV. CONCLUSIONS

From the present study, it was determined that our thin films of the ternary alloy $Ga_5Se_{20}Te_{75}$ are semiconducting. The difference in resistance variation with temperature during the initial heating and subsequent cooling (and also heating) was attributed to the annealing out of frozen-in defects incorporated during the film growth. The activation energy for conduction was calculated for different film thicknesses and it appears to be mildly thickness dependent in the case of thinner films. It is further found that there exists a linear relationship between the resistance of the annealed films and their inverse thickness as expected from the classical size effect theory. From these linear plots, the mean free path values of the charge carriers at different temperatures have been evaluated.

EDAX showed some difference between the film composition and the bulk source material used for the film deposition. XPS revealed the presence of tellurium as tellurium oxide on the surface of the thin film sample. The incorporation of the elements selenium [BE $(3d)=55.5$ eV) and of gallium in traces $(2p_{3/2}=1117$ eV)] in the thin films was also identified by XPS. X-ray diffractograms confirm that the films are of single phase GaSeTe alloy and no oxides or pure elements are present in the films.

ACKNOWLEDGMENTS

One of the authors (K.S.R.) thanks Professor J M Honig of Chemistry Department and Professor Delgauss of Chemical Engineering Department, Purdue University, West Lafayette, USA, for their encouragement and facilities and to R. J. Smiley for the assistance with ESCA.

[1] S. R. Ovshinsky, Phys. Rev. Lett. **21**, 1450 (1968).
[2] N. F. Mott, Philos. Mag. **24**, 911 (1971).
[3] Y. S. Chiang and J. K. Johnson, J. Appl. Phys. **38**, 1647 (1967).
[4] J. Feinleib, J. P. de Neufville, S. C. Moss, and S. R. Ovshinsky, Appl. Phys. Lett. **18**, 254 (1971).
[5] K. S. Kim and D. Turnbull, J. Appl. Phys. **44**, 5237 (1973).
[6] D. W. Vance, J. Appl. Phys. **42**, 5430 (1971).
[7] N. F. Mott and E. A. Davis, *Electronic Processes in Non-crystalline Materials* (Clarendon, Oxford, 1979).
[8] H. K. Henisch, Thin Solid Films **83**, 217 (1981).
[9] J. C. Rhee, M. Okuda, and T. Matsushita Jpn. J. Appl. Phys. **26**, 102 (1987).
[10] H. Fukumoto, K. Tsunetomo, T. Imura, and Y. Osaka, J. Phys. Soc. Jpn. **56**, 158 (1987).
[11] M. Terao, S. Horigome, K. Shigematsu, Y. Miyauchi, and M. Nakazawa J. Appl. Phys. **62**, 1029 (1987).
[12] D. P. Gosain, M. Nakamura, T. Shimizu, M. Suzuki, and S. Okano, Jpn. J. Appl. Phys. **28**, 1013 (1989).
[13] M. Okuda, F. S. Jiang, J. C. Rhee, H. Takenoshita, and O. Matsushita, Appl. Surf. Sci. **33,34**, 797 (1988).
[14] V. Damodara Das and P. Jansi Lakshmi, Phys. Rev. B **37**, 720 (1988).
[15] V. Damodara Das, S. Aruna, and K. S. Raju, *Physics and Technology of Semiconductor Devices and Integrated Circuits*, SPIE Publication, Vol. 1523, p. 271–276, (1992) (Tata-McGraw Hill, New Delhi, 1992).
[16] V. Damodara Das, K. S. Raju, and A. Bhaskaran, *Physics of Semiconductor Devices*, edited by Krishan Lal (Narosa, New Delhi, 1993) pp. 483–485.
[17] L. I. Maissel, in *Handbook of Thin Film Technology*, edited by L. I. Maissel and R. Glang (McGraw Hill, New York, 1970), pp. 13–26.
[18] V. Vand, Proc. Phys. Soc. (London) **55**, 222 (1943).
[19] W. Primak, Phys. Rev. **100**, 1677 (1955).
[20] C. J. Meechan and Brinkman, Phys. Rev. **103**, 1193 (1956).
[21] V. Damodara Das, J. Appl. Phys. **55**, 1023 (1984).
[22] V. Damodara Das and Anand S. Talwai, Thin Solid Films **81**, 21 (1981).
[23] V. Damodara Das and N. Jayaprakash, J. Vac. Sci. Technol. **20**, 58 (1982).
[24] K. Fuchs, Proc. Cambridge Philos. Soc. **34**, 100 (1938).
[25] E. H. Sondheimer, Adv. Phys. **1**, 1 (1952).
[26] A. F. Mayadas and M. Shatzkes, Phys. Rev. B **1**, 1382 (1970).
[27] C. R. Tellier and A. J. Tosser, Thin Solids Films **42**, L31 (1977).
[28] F. Warkusz, Thin Solids Films **52**, L9 (1978).
[29] C. D. Wagner, W. M. Riggs, L. E. Davis, and G. E. Mullenberg, *Hand Book of X-ray Photoelectron Spectroscopy* (Perkin Elmer, 1978), pp. 182–185.